eLife

Reviewed Preprint
v1 • June 12, 2026
Not revised

For correspondence:
yang.bai@siat.ac.cn
xiongfei.fu@siat.ac.cn

* These authors contributed equally to this work.

Competing interests: The authors declare no competing interests

Funding: See page 17

Reviewing editor: Agnese Seminara, University of Genoa, Italy

Optimal chemotactic navigation in disordered landscapes

Yang Bai[1,2,*], Caiyun He[1,2,*], Weirong Liu[1,2], Songtao Cheng[1,2], Pan Chu[1,2], Liang Luo[3], Chenli Liu[1,2], Xiongfei Fu[1,2]

[1]State Key Laboratory for Quantitative Synthetic Biology, Shenzhen Institute of Synthetic Biology, Shenzhen Institutes of Advanced Technology, Chinese Academy of Sciences, Shenzhen, China • [2]University of Chinese Academy of Sciences, Beijing, China • [3]Huazhong Agricultural University, Wuhan, China

eLife Assessment

This **useful** study examines how the swimming of a lab strain of Escherichia coli changes under laboratory conditions designed to mimic disordered, porous environments: a setting that is biologically relevant and less understood than chemotaxis in bulk liquid. By combining experimental evolution in soft agar, inducible control of run duration, visualization of flagella, and theoretical modeling, the authors demonstrate that the optimal mean run duration for migration in semisolid agar is substantially shorter than in liquid and decreases with increasing agar concentration. The authors provide **incomplete** evidence regarding optimal chemotaxis in porous media as emerging through evolution from tradeoffs that involve newly discovered trapped states.

https://doi.org/10.7554/eLife.110412.1.sa3

Abstract

Active navigation in disordered media depends on a biased random walk interacting with environmental constraints. Using *E. coli* chemotactic navigation in agar gels as a model system, we reveal a fundamental trade-off between diffusive exploration and chemotactic directional bias that dictates the optimal strategy for population range expansion. Counter-intuitively, evolution selects for shorter mean run times (τ_f) to achieve faster chemotactic migration in denser environments. Controlled experiments reveal a non-monotonic relationship between chemotactic navigation speed and τ_f, with the optimum shifting according to the density of physical traps in the gel. Single-cell analysis demonstrates that escape from these traps occurs independently of the tumbling mechanism, challenging the classical view that reorientation is essential for navigation in obstructed spaces. Based on these insights, we develop a minimal theoretical model showing that the optimal τ_f emerges from an antagonistic scaling: while the diffusion coefficient increases with τ_f, the chemotactic bias coefficient decreases with it. This work establishes a general principle for optimizing active transport through complex, disordered environments.

Introduction

Bacteria navigate dynamic environments by actively modulating their run-and-tumble motility, a fundamental mechanism for sensing and responding to chemical gradients, known as chemotaxis[1–8]. This locomotion alternates between directed movement (“runs”), propelled by rotating flagellar bundles, and stochastic reorientation (“tumbles”), which randomize the cell’s direction[9–15]. By adjusting run duration in response to temporal changes in attractant concentration, bacterial cells bias their motion to migrate directionally along chemical gradients[9,16–19].

In homogeneous liquid environments, the chemotactic ability (χ) of a bacterium is often proportional to its translational diffusion coefficient *(D)* [1,20–23], which is intrinsically set by the mean free runtime, τ_f. However, in natural habitats such as soil, porous gels, or mucous layers, bacteria encounter disordered landscapes where physical obstacles act as transient traps[24–27]. These obstacles confine motility, introducing an external trapping timescale, τ_t, that operates alongside the intrinsic tumbling timescale. While theoretical and experimental studies have examined how this interplay affects diffusive transport[24,26,28–30], a critical question remains: how does it fundamentally shape chemotactic searching and navigation strategies?

Resolving this question is critical because chemotaxis often enables far more effective population expansion than simple passive diffusion. Bacterial groups can dynamically generate their own chemoattractant gradients by metabolizing local resources, facilitating coordinated migration and rapid colonization that outstrips classical growth-diffusion dynamics[1,7]. This capability confers a significant evolutionary advantage. Consequently, a central question arises: how do bacteria optimize their intrinsic motility parameters, such as τ_f, to maximize navigation efficiency under external constraints of a disordered landscape (Fig. S1)? Understanding this adaptive optimization is key to deciphering microbial ecology and holds promise for applications in bioremediation and synthetic biology.

In this work, we investigate how bacteria optimize chemotactic navigation in disordered environments. Through experimental evolution, we identified a density-dependent optimal mean free run time (τ_f^{opt}) that maximizes the population chemotacitc navigation speed. Using a strain with titratable τ_f, we demonstrate a non-monotonic relationship between the chemotactic navigation speed and τ_f, where τ_f^{opt} shifts according to environmental trap density. Single-cell tracking reveals that trapping-escaping events are unbiased, with escapes occurring independently of tumbling. Motivated by this observation, we developed a theoretical model showing that while prolonged runs enhance diffusion, they paradoxically suppress chemotactic bias in disordered media. This trade-off between directional bias and diffusive exploration explains the observed non-monotonic dependence of chemotactic performance on τ_f. Our findings elucidate a key adaptive strategy by which bacteria tune their motility, balancing exploration and trapping to navigate complex environments.

Results

Phenotypic evolution of chemotactic bacteria in agar gels

To understand how chemotactic bacteria adapt to disordered environments, we performed a spatial evolution experiment selecting for rapid range expansion in *E. coli* MG1655 populations[31–33]. We propagated populations on semi-solid agar plates at two concentrations (0.2% and 0.3%), which modulate the gel's pore size and density, thereby creating random traps that impede bacterial motility[34]. Bacteria were inoculated at the center of each plate; nutrient consumption generated self-generated chemoattractant gradients that drove outward migration. After 24 hours —sufficient for full plate colonization—we transferred cells from the migration front to a fresh plate, repeating this selection process over 40 cycles (~500 generations) (Fig. 1a).

We quantified the chemotactic navigation by imaging the expansion front, which advanced linearly with time. Over successive cycles, evolved populations at both agar concentrations exhibited a progressive increase in chemotactic navigation (Fig. 1b). Crucially, the growth rate of the evolving populations, measured every 5 cycles, remained constant throughout the experiment (see Methods and Fig. S2a). Given that chemotactic navigation is governed by the chemotaxis coefficient (χ) when growth rate is unchanged[1], these results indicate that selection specifically enhanced chemotactic performance in these obstructed environments.

To identify the mechanistic basis of this adaptation, we analyzed single-cell trajectories of evolved populations using a customized tracking platform[8,18,19,35]. This revealed agar concentration-dependent shifts in motility parameters. Cells evolved in higher-concentration agar (0.3%) exhibited a shorter mean free run time (τ_f) and mean free run length compared to those evolved at 0.2% (Fig. 2c, Fig. S2b). Notably, the tumble duration (τ_{tmb}) and mean run speed (v_0)

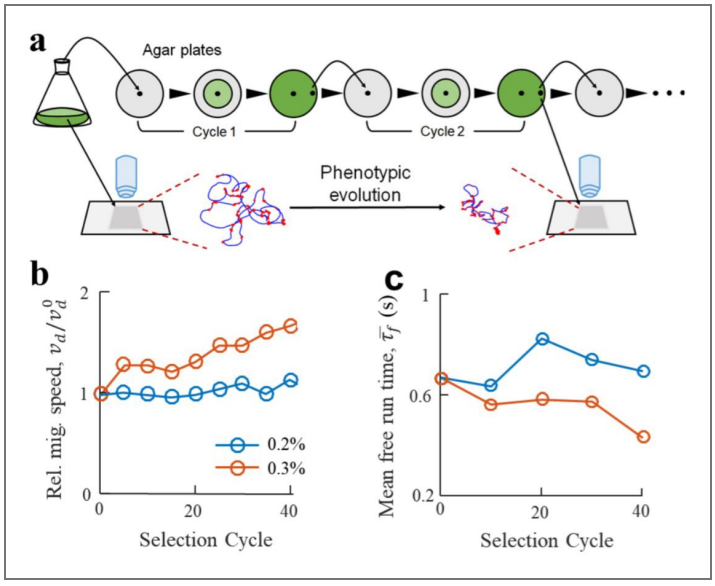

Figure.1. Phenotypic evolution of bacterial chemotaxis in disordered landscapes.

(a) Schematic of the experimental evolution protocol for selecting rapid chemotactic navigation in semi-solid agar gels. (b) Chemotactic navigation of the evolving populations as a function of selection cycle for the two agar concentrations. (c) The average intrinsic free run time τ_f of evolved populations, measured in liquid medium, converges to distinct, agar concentration-dependent values. Populations evolved in denser gels (0.3% agar) adapt a shorter optimal τ_f.

remained constant across all conditions (Fig. S2c,d). Consequently, tumble bias increased accordingly (Fig. S2e). Key motility parameters of the evolved strains including run times, run lengths, and tumble durations, retained Poisson-distributed dynamics after 40 evolutionary cycles (Fig. S3a-c). Meanwhile, tumble bias and run speed exhibited unimodal distributions after evolution (Fig. S3d,f), indicating that evolutionary tuning of τ_f occurred without destabilizing the core chemotaxis regulatory network[22,23].

Together, these findings demonstrate that adaptation to disordered landscapes involves the precise modulation of the intrinsic run time, τ_f. This evolutionary tuning optimizes motility by balancing the exploratory benefit of long runs against the increased risk of trapping. This raises a central question: how does environmental trap density mechanistically define the optimal mean free run time for efficient chemotactic navigation?

Non-monotonic dependence of chemotactic navigation on run time

The evolutionary tuning of τ_f suggests the existence of an optimal free runtime τ_f^{opt} for bacterial chemotactic navigation in disordered landscapes. To test this hypothesis, we used a τ_f titratable strain in which τ_f increases linearly with the logarithm of the external inducer (aTc) concentration (Fig. 2a & Methods). Using this strain, we measured the population chemotactic navigation (V_d) in agar gels of 0.2% and 0.3%. We observed a pronounced non-monotonic dependence of V_d on τ_f: the speed initially increased with longer run times but declined after surpassing a distinct optimum τ_f^{opt} (Fig.2b). This non-monotonic dependence implies a fundamental trade-off: while prolonged runs enhance diffusion exploration and gradient sensing in open environments, they concurrently increase the probability of becoming trapped in a disordered landscape that penetrates chemotactic navigation.

Critically, the value of τ_f^{opt} is itself dependent on the properties of the environment. Competition assays revealed that in denser agar (0.3%), τ_f^{opt} shifts to a significantly smaller value than in softer (0.2%) agar (Fig. S4).

This inverse relationship between τ_f^{opt} and gel density allowed strains with τ_f^{opt} values closer to the environment-specific τ_f^{opt} to gain a selective advantage during range expansion. These results are in qualitative agreement with our evolutionary trajectories (Fig. 1c), confirming that selection drives populations toward the τ_f that maximizes the chemotactic navigation in a given landscape [7,33]. The discrepancy between the measured τ_f^{opt} (Fig. 2b) and the τ_f in evolved strains in Fig. 1c can be partially attributed to the concurrent evolution of mean swimming speed which enabled evolved strains to cover a longer distance within the same time interval (Fig. S2d).

Bacterial motion within random traps

To elucidate bacterial navigation in porous hydrogels, we sought to distinguish intrinsic behavioral states—running and tumbling—from extrinsic immobilization caused by physical confinement (trapping). In *E. coli*, running is driven by the rotation of a bundled flagellar motor, while tumbling is triggered by flagellar unbundling. We hypothesized that a third state exists: cells with bundled flagella that are physically arrested by the gel matrix. To differentiate these states, we employed an *E. coli* strain with modified FliC proteins, enabling specific fluorescent labeling of flagella[15] (Fig. 3a & Methods).

Using high-resolution time-lapse fluorescence microscopy, we simultaneously tracked flagellar dynamics and cellular trajectories (Fig. 3b, Movies S1 and S2). A custom machine-learning pipeline, based on the YOLOv5 architecture, was trained to automatically classify flagellar configurations as “bundled” or “split” states (Fig. 3c, left). Instantaneous swimming velocities were computed and normalized to the 95th percentile speed of each trajectory to account for cell-to-cell variability[8] (see Methods). This revealed a distinct bimodal velocity distribution for the bundled state in agar, contrasting with the unimodal distribution in liquid. A new peak emerged near zero velocity, corresponding to cells with active, bundled flagella whose motion was

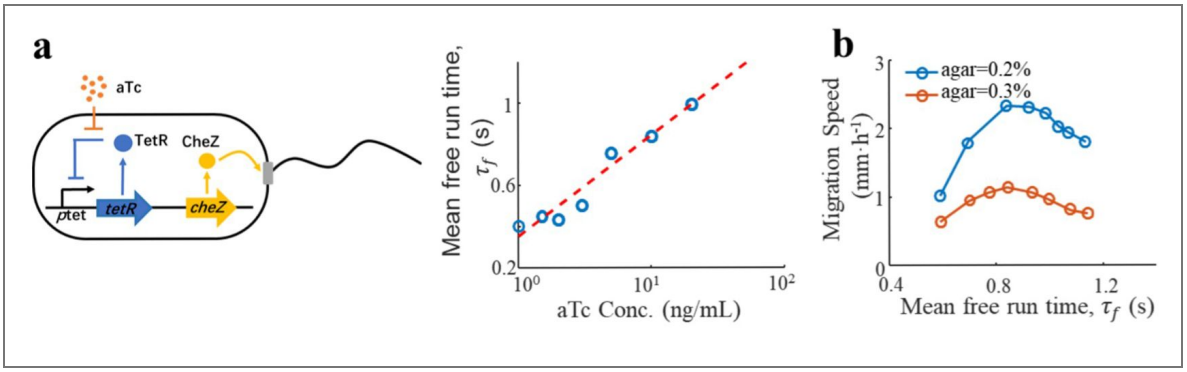

Figure 2. Non-monotonic navigation speed reveals an optimal run time.

(a) Design and validation of the τ_f-titratable strain. Left: Genetic circuit for anhydrotetracycline (aTc)-inducible control of *cheZ* expression. Right: The mean free run time (τ_f) of the engineered strain increases linearly with the logarithm of the aTc concentration. (dashed red line is the linear fit). More than 8000 cells were tracked at each aTc concentration, the standard error of the mean (SEM) of τ_f is smaller than marker size in all conditions. (b) Chemotactic navigation exhibits a non-monotonic dependence on the intrinsic free run time. Three replicates were performed for each condition with error smaller than marker size. The optimal free run time that maximizes chemotactic navigation is larger in 0.3% agar than in 0.2% agar.

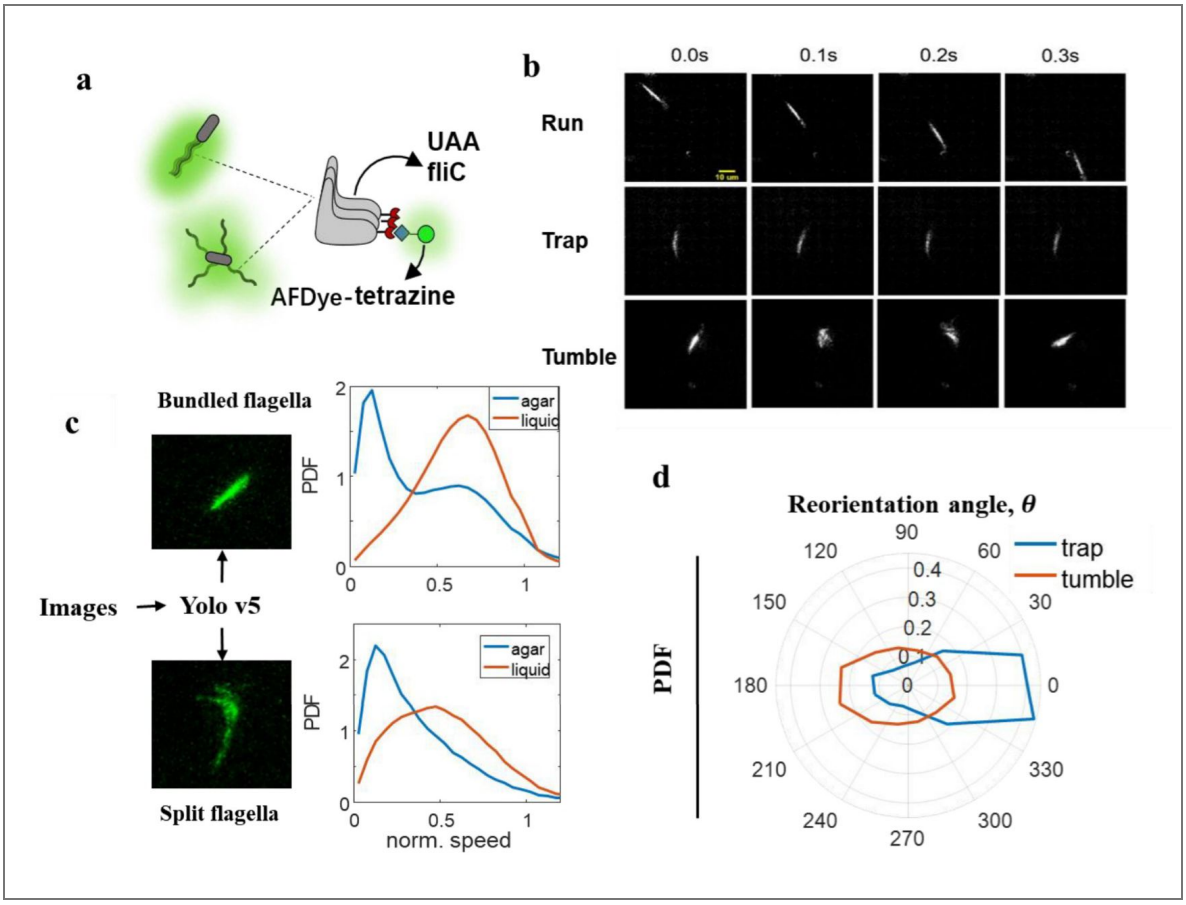

Figure 3. Single-cell analysis of bacterial motility.

(a) Fluorescent labeling of bacterial flagella is achieved by incorporating an unnatural amino acid (UAA) into the FliC protein, followed by conjugation with AFDye-tetrazine, enables visualization of flagellar structure and dynamics. (b) Representative fluorescence time-laps micrograph of an *E. coli* cell embedded in a 0.2% agar gel, showing three distinct behavioral states: Run (cell in motion with bundled flagella); Trap (cell stopped with bundled flagella); Tumble (cell stopped with split flagella). (c) Left: Representative image frames with cells automatically identified and classified as having bundled or split flagella using an in-house trained YOLOv5 detection model. Right: Cells were tracked across frames to reconstruct trajectories, and velocities were calculated and annotated with corresponding flagellar states. The normalized swimming speed (normalized to the 95th percentile speed of each individual trajectory) is displayed as probability density distributions for each flagellar configuration: bundled (running or trapped) and split (tumbling), in both liquid medium (red curves) and in 0.2% agar gel (blue curves), revealing distinct motility dynamics across environments. (d) Probability density functions (PDF) of reorientation angles following tumbling (red) and trapping (blue) events in agar (see Methods).

physically restrained by the gel—defining the "trapped" state (Fig. 3c, right). By integrating flagellar morphology classification with a dual Gaussian distribution model to differentiate between states, we resolved three distinct motility states within individual trajectories: running, tumbling, and trapping (Fig. S5a).

We next investigated the kinetics of these states. Run and tumble durations followed exponential distributions, consistent with memoryless, intrinsic stochastic processes. In stark contrast, trapping durations exhibited a stretched exponential distribution with a heavy tail (Fig. S5b), indicating heterogeneous escape kinetics governed by variations in local pore geometry. To determine the escape mechanism from traps, we analyzed over 9,000 run-trap-run transitions. Only 295 of these escapes (<3%) were associated with a tumble event, demonstrating that tumbling is not the primary escape mechanism. We quantified directional persistence by measuring the angular change between the incoming and outgoing run directions. While post-tumble reorientation angles were uniformly distributed, angles following trap release showed a strong bias toward the original direction of motion (Fig. 3d).

This pronounced asymmetry reveals that the agar gel does not function as a rigid barrier. Instead, bacteria appear to navigate around or through transient, deformable traps without significantly altering their heading or relying on tumbling to execute detours. This observation challenges the classical view— supported by studies in rigid polymer environments—that bacteria primarily rely on tumbling to escape confinement and reorient[29,36–38]. Consequently, our findings redefine the role of tumbling in confined landscapes: rather than serving as an essential escape mechanism, tumbling appears to play a more nuanced role in the broader chemotactic strategy within disordered environments.

Modeling bacterial chemotaxis in disordered landscapes

Informed by our single-cell characterization of trapping and tumbling events (Fig.3 & Fig. S5), we model bacterial motility in disordered landscapes as a combination of two independent stochastic processes: run-tumble and run-trap dynamics (Fig. 4a). The intrinsic run-tumble process is governed by switching rates λ_{rt} (run to tumble) and λ_{tr} (tumble to run), which define the mean free run time $\tau_f = 1/\lambda_{rt}$ and the mean tumble duration $\tau_{tmb} = 1/\lambda_{tr}$. Simultaneously, the extrinsic run-trap process interrupt runs at a rate r_{rt} ($\tau_t = 1/r_{rt}$, mean runtime between traps) and detain cells for a mean trapping time $\tau_{trp} = 1/r_{tr}$. The effective duration of an uninterrupted run in the gel, τ_R, is thus determined by the combined probability of intrinsic tumbling and extrinsic trapping: $\tau_R = \left(\tau_f^{-1} + \tau_t^{-1}\right)^{-1}$.

Assuming, for simplicity, uniform reorientation angles for both tumbling and trapping events, the diffusion coefficient D in a 1D system is given by: $D = \frac{v_0^2}{2}\frac{\tau_R^2}{\tau_R+\tau_S}$, where v_0 is the run speed and τ_S is the mean stop time, $\tau_S = P_{tmb}\text{-}\tau_{tmb} + P_{trp}\text{-}\tau_{trp}$, with probabilities $P_{tmb} = \tau_f^{-1}\left(\tau_f^{-1} + \tau_t^{-1}\right)^{-1}$ and $P_{trp} = \tau_t^{-1}\left(\tau_f^{-1} + \tau_t^{-1}\right)^{-1}$. For a fixed trapping time τ_{trp} at a given agar concentration, this model predicts the diffusion coefficient D increases monotonically with τ_f(Fig. 4b). Crucially, because trapping events do not induce a directional bias (negative reorientation angles, Fig. 4d), this model alone cannot explain the non-monotonic behavior observed in our experiments, in contrast to previous models that proposed tumbling as a mechanism for bacteria to escape traps [29,36,39].

To elucidate the non-monotonic relationship between chemotactic navigation speed (χ) and mean free runtime (τ_f), we introduced biased runs to model chemotaxis in agar gels. Cells extend their runs when moving up gradients (τ_f^+) and shorten them when moving down (τ_f^-) (Fig. 4c). Reflecting the fundamental principle of bacterial chemotaxis with sensory adaptation[40–42], we assume runtime deviation ($\delta\tau_f$) is proportional to mean free runtime: $\delta\tau_f \equiv \tau_f^+ - \tau_f \equiv \tau_f - \tau_f^- = \alpha G\tau_f$, where α is a constant representing the strength of the internal chemotactic response and G denotes the external chemoattractant gradient. The effective free runtimes in gradient-aligned (±) directions becomes $\tau_R^{\pm} = \frac{\tau_f^{\pm}\tau_t}{\tau_f^{\pm}+\tau_t}$.

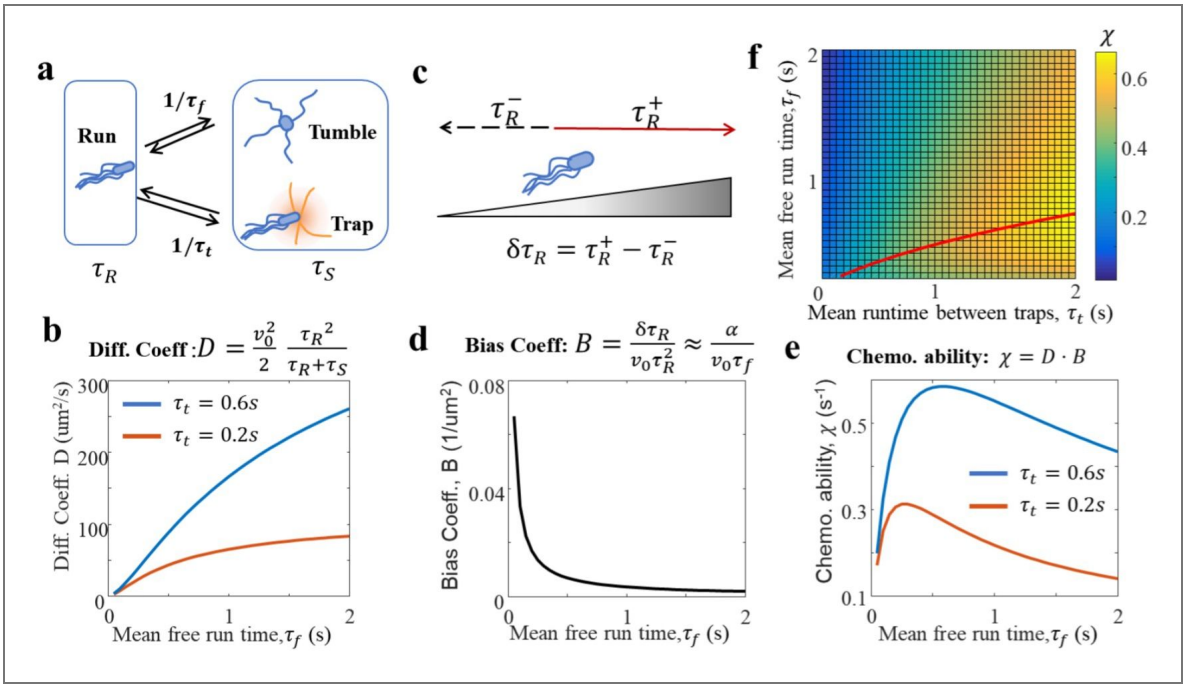

Figure 4. A minimal model reveals a diffusion-bias trade-off.

(a) Schematic of the stochastic model combining intrinsic run-and-tumble dynamics with extrinsic trapping by the environment. (b) Predicted diffusion coefficient *D* as a function of the intrinsic mean free run time τ_f for different mean trap intervals τ_t. In the absence of a chemo-attractant gradient, *D* increases monotonically with τ_f but is suppressed as the trap density increases (red line: low trap concentration, $\tau_t = 0.6s$; blue line: high trap concentration, $\tau_t = 0.2s$). (c) Modeling chemotaxis: cells extend runs (τ_f^+) when moving up a gradient (blue) and shorten them (τ_f^-) when moving down (red), creating a directional bias. (d) The bias coefficient, representing the deviation of free run durations, decreases with mean free runtime τ_f. (e) the product of the diffusion coefficient and the bias coefficient yields the chemotactic ability χ, which exhibits a non-monotonic dependence on the mean free runtime τ_f. (f) Heatmap of chemotaxis ability χ in the (τ_f,τ_t) parameter space. The optimal mean free runtime τ_f^{opt} as a function of τ_t is shown as a red line. The external gradient *G* was assumed to be $1\mu m^{-1}$ for simplicity.

This asymmetry generates a drift velocity: $V_d = \frac{v_0 \delta\tau_R}{2(\tau_R+\tau_S)}$, where $\delta\tau_R \equiv (\tau_R^+ - \tau_R^-) \approx \frac{\alpha G \tau_f \tau_t^2}{(\tau_f+\tau_t)^2} = \frac{\alpha G}{\tau_f}\tau_R^2$ (see methods), which further defines the chemotaxis ability $\chi = V_d/G \approx \frac{\alpha}{\tau_f}\tau_R^2$. This chemotaxis ability χ can be decomposed into the product of a diffusion coefficient D and a bias coefficient B: $\chi = D \cdot B$, where $B \equiv \frac{\delta\tau_R}{v_0\tau_R^2} \approx \frac{\alpha}{v_0\tau_f}$.

This formulation reveals the core trade-off: while the diffusion coefficient D increases with τ_f (Fig. 4b), the bias coefficient B decreases inversely with τ_f (Fig. 4d). Their product, chemotaxis ability χ, therefore exhibits a maximum at an intermediate optimal mean run time τ_f^{opt} (Fig. 4e). Analytically, this optimum scales with the environmental trapping time: $\tau_f^{opt} = \sqrt{\frac{\tau_{tmb}}{(\tau_t+\tau_{trp})}}\tau_t$ (Fig. 4f & method).

This scaling explains why the evolved τ_f decreases with agar concentrations (Fig. 2c). A phase diagram of $\chi(\tau_t,\tau_f)$ highlights τ_f^{opt} (Fig. 4f), underscoring how environmental constraints shape evolutionary tuning of motility. The observed non-monotonic navigation efficiency thus emerges from a fundamental competition between enhanced diffusion and diminished bias with increasing τ_f. This trade-off defines an adaptive optimum, enabling bacteria to balance exploration and directional sensing in disordered landscapes—a principle that is generalizable to microbial navigation in a wide range of heterogeneous environments.

While this simplified model successfully captures the core trade-off for optimal chemotactic navigation, we also constructed a more rigorous framework incorporating detailed chemotaxis signaling dynamics[11,17,20,42–48]. This model integrates the adaptation dynamics of chemoreceptor free energy with the kinetics of CheY-P concentration and motor rotation, using experimentally measured constants (see Methods). From this, we derive the effective run-time deviation ($\delta\tau_R$) as: $\delta\tau_R \approx \frac{GNv_0^2}{d}\frac{\tau'_{R0}}{(1+\tau_R(F_0)/\tau)}$, where τ is adaptation time of bacterial chemotaxis signaling systems, $\tau'_{R0} \equiv \partial_F \tau_R(F_0)$ reflects sensitivity to chemoattractant gradient, F_0 is the baseline signaling state[20,48]. Numerical simulations confirm the chemotactic navigation speed retains its non-monotonic dependence on τ_f, validating our core theoretical insight (Fig. S6). In this detailed model, the chemotaxis bias (B) decreases with τ_f across biologically relevant regimes, though weak gradient sensing at very low τ_f can introduce a secondary non-monotonic trend.

The non-monotonicity of chemotaxis ability χ can be understood intuitively by considering two asymptotic limits. For long τ_t ($\tau_f \ll \tau_t$), runs are primarily terminated by tumbles ($P_{trp} \ll P_{tmb}$). The bias coefficient B approximates its value in a homogeneous liquid, but the short τ_f severely limits the effective run time τ_R and thus the diffusion coefficient D , constraining overall performance. For short τ_t ($\tau_f \gg \tau_t$), runs are overwhelmingly interrupted by traps ($P_{trp} \gg P_{tmb}$), which impart no directional bias. Consequently, the bias coefficient B — now dominated by rare tumbling events—becomes negligible. Cells thus achieve a high diffusion coefficient but an insignificant drift velocity, rendering them unable to climb gradients effectively.

Discussion

In this study, we demonstrate that bacterial populations evolving under selection for rapid chemotactic navigation in agar gels adapt by tuning their mean free runtime (τ_f), with distinct optimal values (τ_f^{opt}) emerging for different environmental constraints. Using a τ_f-titratable strain, we validated that this evolutionary outcome arises from a non-monotonic relationship between the chemotactic navigation speed and τ_f, where τ_f^{opt} represents a trade-off between diffusion exploration and preserved directional bias. Single-cell tracking with flagellar visualization characterized the bacterial run, trap, and tumble states and revealed that bacteria primarily escape confinement without tumbling or reorientation. By modeling chemotactic navigation as a competition between intrinsic run-tumble and extrinsic run-trap processes, we showed that the non-monotonic chemotaxis ability (χ), emerges from the antagonistic scaling of the diffusion coefficient (D) and the chemotactic bias coefficient (B) with τ_f.

Our findings extend the understanding of bacterial navigation in porous media by examining soft and compliant gels. Whereas studies in rigid hydrogels have highlighted "trapping-hopping" mode that may require active reorientation [24,25,49], our work in softer agar gels reveals that tumbling is not a primary escape strategy[29,36,39], but is instead essential for to generating chemotactic bias. This discrepancy likely stems from material differences: the flexible, transient nature of agar pores permits passive escape via mechanical yielding, whereas rigid environments may necessitate active reorientation to escape immutable traps.

Our work underscores a fundamental distinction between active and passive particles. Passive systems obey linear fluctuation-dissipation relations ($V_D \propto D$), whereas active particles like bacteria can exhibit a non-monotonic relationship between drift velocity and diffusion coefficient. This is a direct consequence of the internal regulation of motility parameters in response to external cues. In contrast, a passive modification of bias, such as by applying an external force G, would yield a monotonic dependence, $V_D \propto G$.

By integrating evolutionary adaptation, single-cell biophysics, and theoretical modeling, we elucidate how bacteria optimize motility parameters to navigate disordered landscapes. Our findings advance the understanding of microbial ecology in porous media (e.g., soils, biofilms) and inform the design of bioengineered systems[7,8,50–52]. Future work could explore how trap geometry and material elasticity modulate τ_f^{opt}, and whether similar principle governs navigation in complex in vivo environments like mucosal layers or tumor microenvironments.

Materials and Methods

Evolution protocol

Exponentially growing E. coli cells MG1655 (ancestor) were inoculated at the center of tryptone medium agar plate with 2different agar concentrations (0.2%, 0.3%). After 24 hour incubation at 37 °C, bacteria colonized the entire plate. 2 μl cell-agar mixture was taken at the edge of the plate (25mm away from the center) and were inoculated at the center of a fresh plate of the same agar concentration. The cycle was repeated for more than 40 times. After each 10 cycles, evolved strains are saved in glycerol stocks. And the motion of the strains are tracked under microscope.

Quantification of bacterial motion in liquid

To quantify the phenotypic variation during the evolution process, evolved bacteria are cultured in tryptone broth and then tracked under microscope with 10X phase contrast object. The tracks were then separated into run stat and tumble stat by a clustering in 3 dimensions (speed, acceleration, and angular velocity) [18]. more than 10,000 cells were tracked in each case, so that the statistics is creditable. The distributions and the cellular averaged values of the run time, run length, tumble times, mean speed, mean run speed are then calculated and plotted in Fig. S2 & Fig. S3.

Chemotactic navigation and competition with CheZ titration strains

we use a synthetic strain that the free runtime is titrated by the expression level of CheZ protein. The titration of CheZ protein was released by introducing negative feedback gene circuit of *ptet-tetR* or *plac-lacI* to replace the original promotor of *cheZ* genes on chromosome as in reference[3]. In these engineered strains, CheZ expression is controlled by externally added inducers (e.g., aTc for the *ptet-tetR* system and IPTG for the *plac-lacI* system), allowing fine-tuned titration of CheZ levels.

To assess the chemotactic performance of this run-time-tunable strain, semisolid agar plates were prepared with varying concentrations of the appropriate inducer (aTc or IPTG) uniformly mixed into the agar. Identical initial cell densities of the strain were inoculated at the center of each plate to ensure consistent and comparable conditions. Bacterial chemotactic navigation was monitored over time using time-lapse camera imaging, and the chemotactic navigation was quantified by tracking the outward movement of the colony edge.

Quantification of bacterial motion in soft agar

To understand how bacteria interact with soft agar, bacteria motions were tracked in agar gels. We first labeled the flagella of bacteria, with the method established in reference[15]. This labelled strain was then cultured in M9 glycerol medium to exponential growing phase, and then was mixed with the prewarmed soft agar medium with corresponding concentration so that the final OD_{600} was 0.04-0.06. 5 ul of this mixture was then dripped on a slide and was sealed by a cover glass. This sample was freezed in 4 °C for 5mins so that the agar solution was congealed. And then was rewarmed in 37 °C for 3mins to reactivate the bacteria before they are tracked under microscope with 60X fluorescent object. So that the flagella conformation was filmed with its position.

Using an algorithm based on YOLO v5, the images of flagella conformation were clustered into 2 stats: bundled or split. With the position of each time point of acquisition, we get the instantaneous velocity. With this information the bacterial motion in agar gel were classified into 3 stats, where run stats with bundled flagella and high velocity; tumble stat with split flagella and low velocity; trap stat with bundled flagella and low velocity.

After identifying the swimming states of bacterial motion, we determined the run time, tumble time, and trap time for each cell in agar gel by counting consecutive segments classified as running, tumbling, or trapped. Cells with short trajectory durations (<5s) or maximal displacements smaller than one flagellar length (< 10 μm) were excluded from the analysis, as they likely represent out-of-focus tracks or tethered cells that do not contribute meaningfully to bacterial chemotactic navigation dynamics.

To quantify reorientation during trapping and tumbling events, we segmented trajectories into distinct motifs: run-trap-run, run-tumble-run, and run-traptumble-run. A comparison of the frequencies of run-trap-run versus run-traptumble-run events revealed that cells typically escape traps without resorting to tumbling. The swimming direction of each run was defined by the vector from its start to end position. The reorientation angle was then computed as the angular difference between the directions of the runs immediately preceding and following each trap or tumble event.

Minimal model of bacterial chemotaxis in disordered landscape

We assume that bacteria control its intrinsic free runtime τ_I by adding or deducting a portion α when going up or down the chemoattractant gradient $\tau_I^{\pm} = \tau_I \pm \delta\tau_I$, with $\delta\tau_I = \alpha\tau_I$. Although simple, this assumption captures the principle of the bacterial chemotaxis strategy. This assumption approximates the more realistic model integrating bacterial chemotaxis pathway. As the biasing factor is small, we can use a Taylor expansion to get the biased effective mean run time of the run-tumble particle:

$$\delta\tau_R = \left|\tau_R^{\pm} - \tau_R\right| \approx \delta\tau_I \cdot \partial\tau_R/\partial\tau_I = \frac{2\alpha G\tau_I\tau_E^2}{(\tau_I+\tau_E)^2}$$

Following this framework, the drift velocity V_d is defined as: $V_d = \frac{v_0}{d}\frac{\tau_R^+ - \tau_R^-}{\tau_R^+ + \tau_R^- + 2\tau_S} = \frac{v_0}{d}\frac{\delta\tau_R}{\tau_R+\tau_S}$, where v_0 is the run speed, d is the dimension factor and $\tau_s = P_{tmb}\tau_{tmb} + P_{trp}\tau_{trp} = \frac{1/\tau_I}{1/\tau_I+1/\tau_E}\tau_{tmb} + \frac{1/\tau_E}{1/\tau_I+1/\tau_E}\tau_{trp}$ defines the mean stop time contributed by weighted tumble time $P_{tmb}\tau_{tmb}$ and trapping time $P_{trp}\tau_{trp}$.

Subscribing the τ_R,τ_S,$\delta\tau_R$ from the model, the drift velocity then simplifies to:

$$V_d \approx \frac{v_0}{d}\frac{\alpha G\tau_I\tau_E^2}{(\tau_I\tau_E + \tau_E\tau_{tmb} + \tau_I\tau_{trp})(\tau_I+\tau_E)}$$

Plotting this drift velocity, we observe non-monotonic dependent on the intrinsic property τ_I at given disordered environment defined by τ_E,τ_{trp} and at fixed tumble time τ_{tmb}.

Complete model with bacterial chemotaxis pathway

The free energy of the receptor then determines the CheY-P concentration *Yp(t)* by $Yp\left(t\right)=\frac{\alpha}{1+e^{F(t)}}$. the switching rate of the bacteria from run stat to tumble stat λ_{rt} and from tumble stat to run stat λ_{tr} writes $\lambda_{rt}=\omega e^{-\left(\frac{g}{4}-\frac{g}{2}\left(\frac{Yp(F)}{Yp(F)+K}\right)\right)}$,$\lambda_{tr}=\omega e^{+\left(\frac{g}{4}-\frac{g}{2}\left(\frac{Yp(F)}{Yp(F)+K}\right)\right)}$, where *ω,g,K* are experimentally measured constants that describe the motor kinetics.

The bacterial receptor's free energy was adapted to an intrinsic value F_0

$$\frac{dF}{dt}=-\frac{1}{\tau_a}\left(F-F_0\right)+\overrightarrow{r}\cdot\overrightarrow{s}v_0NG$$

The run time in agar gel writes:

$$\tau_R=\frac{1}{\frac{1}{\tau_I}+\frac{1}{\tau_E}}$$

with

$$\tau_f=\frac{e^{\left(\frac{g}{4}-\frac{g}{2}\left(\frac{\alpha}{\alpha+K+e^{F(t)}}\right)\right)}}{\omega}$$

At shallow gradient limit where F is close to its steady stat value F_0, one may get:

$$\tau_R^+-\tau_R^-=\frac{2\tau'_{R0}GNv_0}{\left(\frac{1}{\tau}+\frac{1}{\tau_{R0}}\right)}$$

The drift velocity writes:

$$V_d=\frac{v_0}{d}\frac{\tau_R^+-\tau_R^-}{2\tau_{R0}+2\tau_{S0}}\approx\frac{Nv_0^2G}{d}\frac{\tau'_{R0}}{\left(1+\frac{\tau_{R0}}{\tau}\right)}\frac{\tau_{R0}}{\tau_{R0}+\tau_{S0}}$$

These results confirms that the optimal navigation strategy of bacteria on disordered landscape requires a match between the innate free runtime τ_f and the mean free runtime between traps τ_t. Cells with smaller τ_f didn't use up all the free space that the environment allows it; Cells with larger τ_I has almost the same same runtime whether go up or down the gradient as they are trapped to a smaller free runtime defined by τ_E. This effect was more clearly illustrated by the response curve of $\tau_{R0}(F)$ as the climbing or sliding gradient modifies the internal free energy F by a linear manner.

Supplementary figures

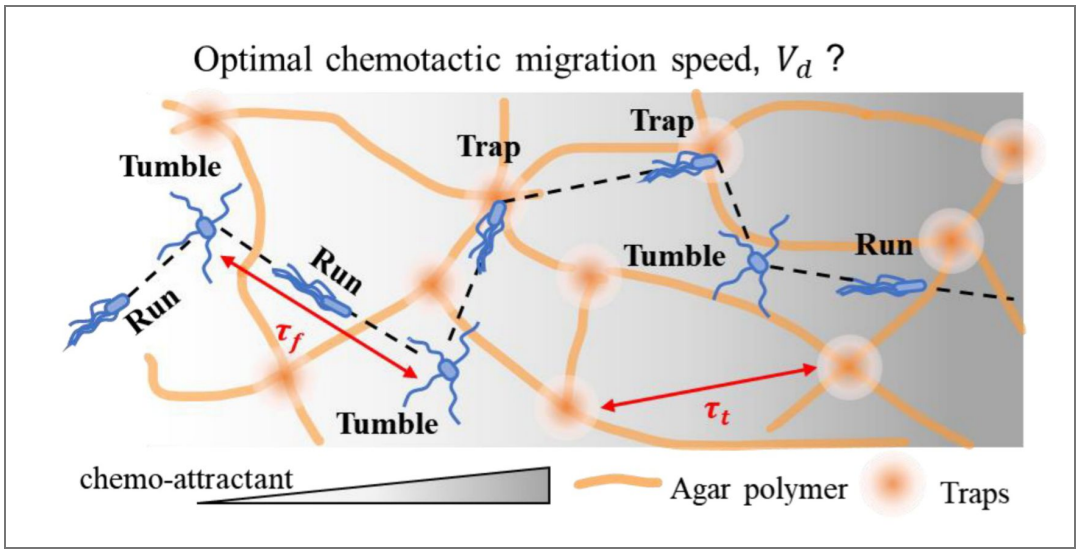

Figure S1. Schematic illustration of bacterial chemotaxis in a porous agar gel environment. This diagram depicts the movement of *E. coli* through a network of pores in agar gel, highlighting the three primary behavioral states: run (straight swimming with bundled flagella), tumble (reorientation via flagellar unbundling), and trap (a newly identified state where cells become temporarily immobilized due to physical confinement). The mean run duration between successive tumbles (τ_f) and mean run duration between successive traps (τ_t) are indicated by red arrows, representing key parameters governing motility dynamics. The orange lines represent the pore structure of the gel, while the gray background denote chemoattractant gradients. This spatially constrained environment imposes selective pressures on motility strategies of bacterial and raises questions on the optimal chemotactic navigation strategy to maximize the chemotactic navigation V_d in porous agar gel.

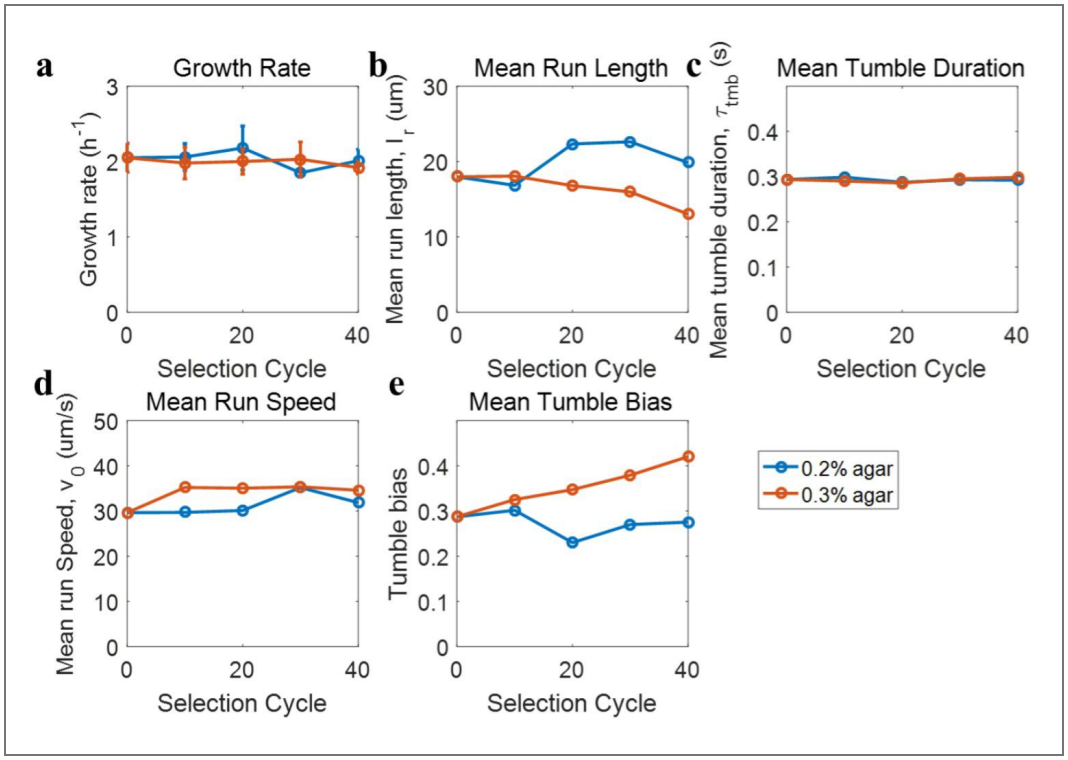

Figure S2. Evolutionary dynamics of motility and growth parameters in liquid culture across selection cycles.

Time courses of key phenotypic traits as measured in evolved E. coli populations over 40 selection cycles under two agar concentrations (0.2% and 0.3%). (a) Growth rates remain stable throughout the selection process, where error bars represent std of 3 independent measurements. (b) Mean run length declines slightly in the 0.3% agar line. (c, d) Tumble duration and mean run speed are maintained at a consistent level across cycles. (e) Tumble bias increases steadily in the 0.3% agar line, while remaining relatively constant in the 0.2% line. Motility related data represent averages from more than 4,800 individual cell tracks and over 100,000 run or tumble events per condition, with standard errors of the mean (SEM) smaller than the symbol size.

Figure S3. Distributions of key motility parameters in evolved strains compared to the ancestral population.

Probability density functions (PDFs) depict five fundamental motility traits measured for the ancestral strain (black lines) and two independently evolved lines selected under 0.2% (blue lines) and 0.3% (red lines) agar concentrations, with data collected from over 100,000 run or tumble events per condition. Panels (a-c) illustrate that distributions of run times, run lengths, and tumble durations all exhibit approximately exponential decay across all strains, indicating consistent stochastic processes underlying these traits. In contrast, panels (d) and (e) show that tumble bias and mean run speed are unimodally distributed, suggesting selective pressures lead to more uniform adaptations in these parameters

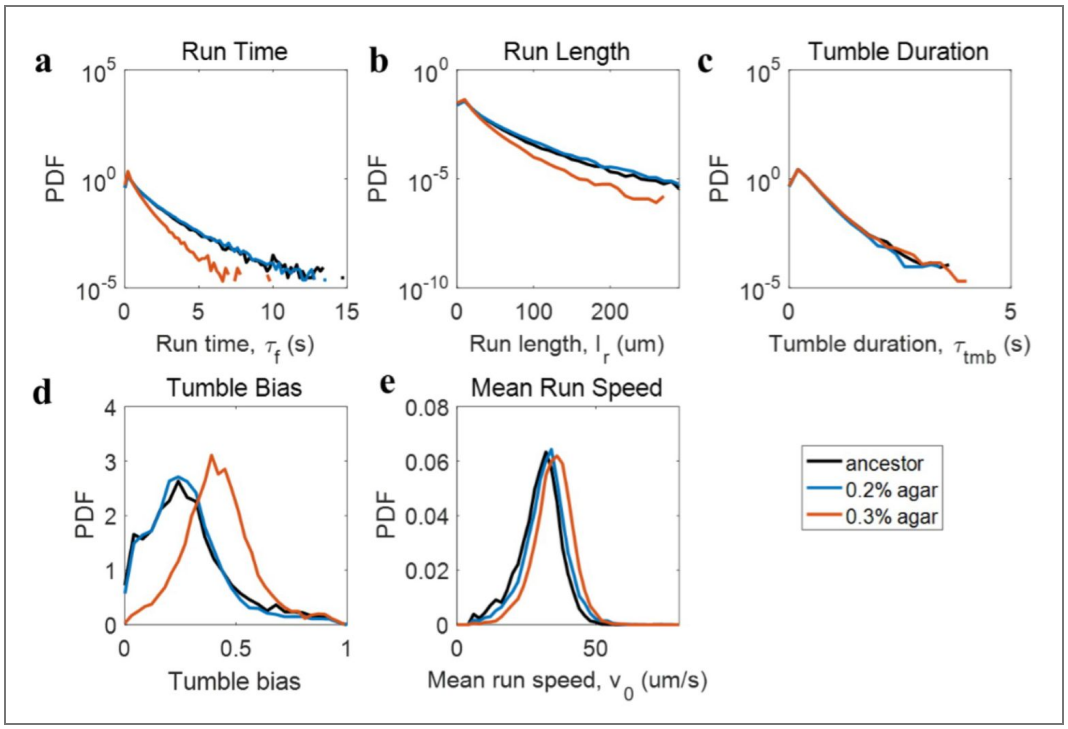

Figure S4. Competitive fitness assay reveals environment-dependent selection of optimal run duration (τ_f).

(a) Schematic representation of two genetically engineered E. coli strains, each with distinct inducible control over the mean run duration (τ_f), achieved via independent expression of CheY from the tetR and lacI systems using aTc and iPTG, respectively. The strains are fluorescently labeled (green and red) for spatial tracking during competition. (b,c) Competitive range expansion assays on 0.2% agar (b) and 0.3% agar (c), where both strains were co-inoculated at equal initial density and allowed to expand overnight at 37 °C. Fluorescence imaging reveals the spatial distribution of each strain across the expanding colony. On 0.2% agar (b) the green one dominates the outer edge of the colony, indicating superior dispersal in less confined environments. In contrast, on 0.3% agar (c), this red strain is enriched toward the center expands outward, demonstrating that shorter run durations are favored under higher physical confinement.

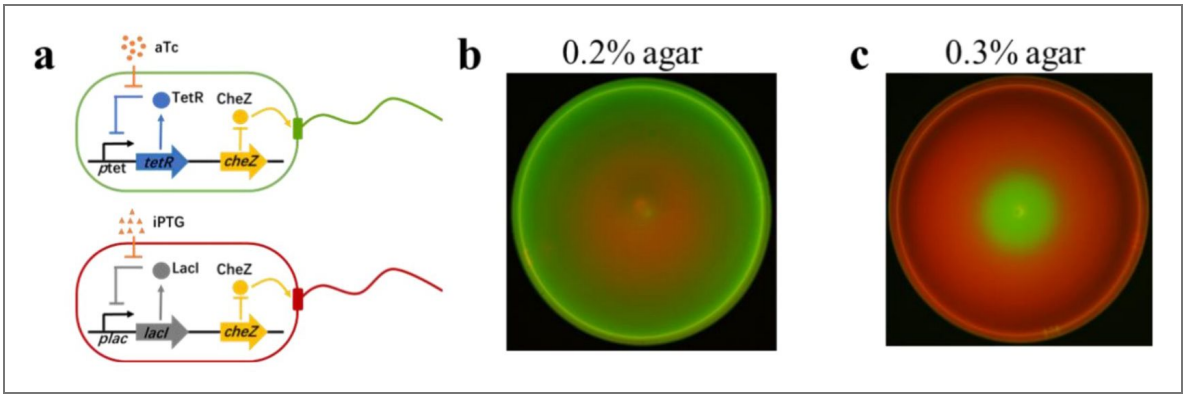

Figure S5. **Motility behavior of *E. coli* in agar gel.**

(a) Representative trajectory of a single bacterial cell moving through a 0.2% agar gel, with automatically detected behavioral states annotated: runs (blue line), tumbles (red dots), and traps (green dots). The trajectory reveals frequent reorientations and prolonged pauses indicative of physical confinement and interaction with the gel matrix. (b) Probability density functions (PDFs) of the duration for run, tumble, and trap events in 0.2% agar gel, showing distinct temporal signatures. Runs exhibit a broad exponential decay, consistent with stochastic motility, while tumbles are brief and sharply peaked. Trap durations are longer and more variable, reflecting transient immobilization due to pore entrapment.

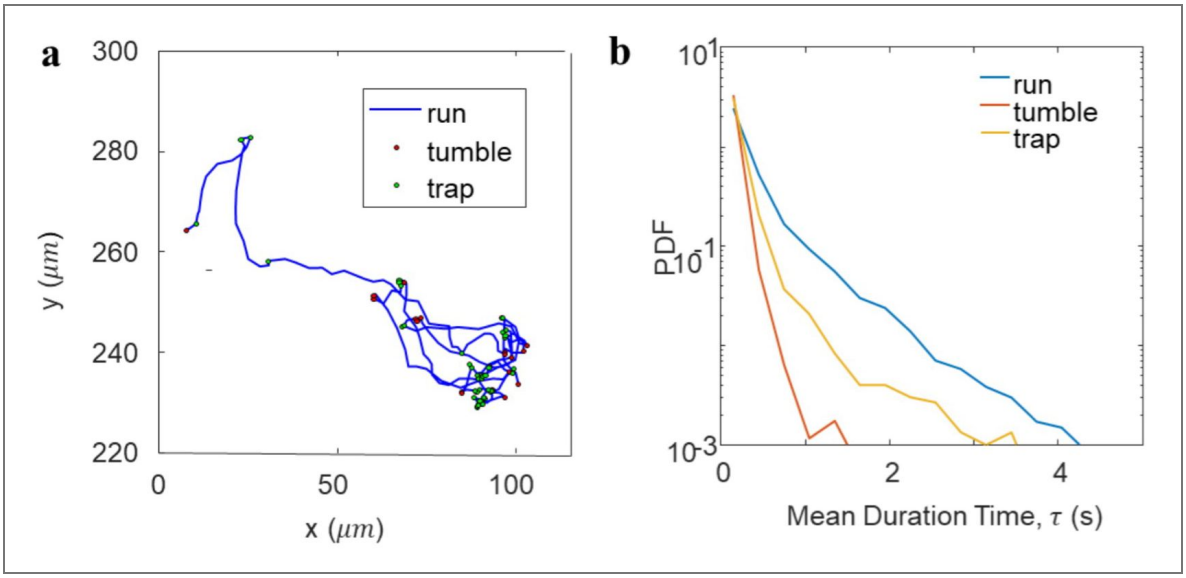

Figure S6. **Prediction of the model with complete chemotaxis pathway.**

Simulations incorporating the full bacterial chemotaxis network reveal how key motility metrics depend on the mean trap intervals τ_t and intrinsic run duration τ_f. (a) Effective drift velocity in a chemoattractant gradient peak at intermediate values of τ_f, with optimal chemotaxis occurring when τ_f is tuned relative to τ_t(black line). (b) Contour plot of chemotactic ability (χ) across a range of τ_f and τ_t, revealing an increasing trend of τ_f^{opt} over τ_t. This predicted dependence decreases with agar concentration, in quantitative agreement with experimentally observed behavioral (Fig. 1c and Fig. 2b).

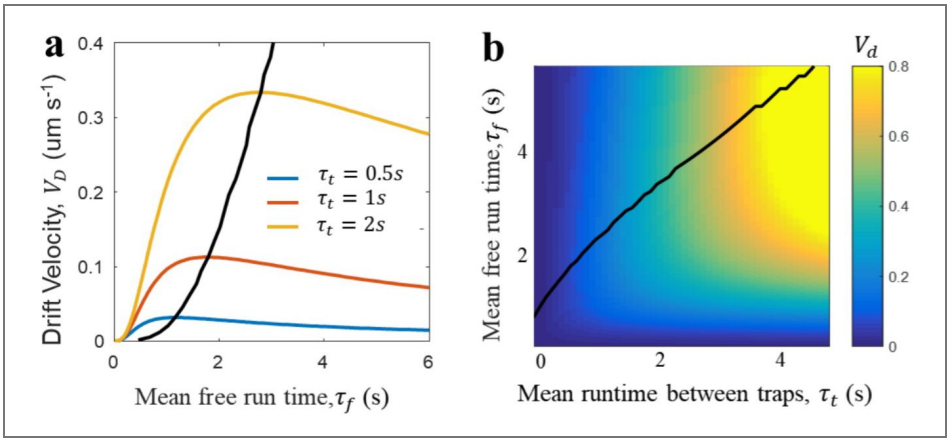

Data availability

All data required to support this article is available in Zenodo at *https://zenodo.org/records/17475731*.

Acknowledgements

This work is partially supported by NSFC (T2525031, 32571666, 32371492), the National Key Research and Development Program of China (2024YFA0919600, 2021YFA0910703), Strategic Priority Research Program of Chinese Academy of Sciences (XDB0480000), and General Project of Basic Research under the Shenzhen Science and Technology Plan (JCYJ20230807140810022), Natural Science Foundation of Guangdong Province, China (2025A1515011919).

Additional information

Author contribution

Y. Bai & X. Fu initiated this project; Y. Bai performed the data analysis and theory deduction; C. He imaged single cell behavior in agar gel, quantified the migration rate of titrated cells and performed the competition assay; W. Liu performed the directed evolution of bacteria; S. Cheng helped in single cell imaging and analysis; P. Chu helped to construct the titration strain; L. Luo helped in the theory deduction.

Funding

Funder	Grant reference number	Author
MOST | National Natural Science Foundation of China (NSFC)	T2525031	Xiongfei Fu
MOST | National Natural Science Foundation of China (NSFC)	32571666	Yang Bai
MOST | National Natural Science Foundation of China (NSFC)	32371492	Weirong LIU
MOST | National Key Research and Development Program of China (NKPs)	2024YFA0919600	Xiongfei Fu
MOST | National Key Research and Development Program of China (NKPs)	2021YFA0910703	Yang Bai
Shenzhen Municipal Science and Technology Innovation Council | Shenzhen Science and Technology Innovation Program	JCYJ20230807140810022	Caiyun He
GDSTC | Natural Science Foundation of Guangdong Province	2025A1515011919	Yang Bai

Author ORCID iDs

Yang Bai: https://orcid.org/0000-0001-9976-2686
Chenli Liu: https://orcid.org/0000-0003-3029-7207
Xiongfei Fu: https://orcid.org/0000-0003-3657-8296

Additional files

Movie S1. Trapping stat of bacteria in agar gel

Movie S2. Tumble stat of bacteria in liquid

References

1. **Narla A. V.,** Cremer J., Hwa T. (2021) A traveling-wave solution for bacterial chemotaxis with growth. *Proc Natl Acad Sci U S A* **118** https://doi.org/10.1073/pnas.2105138118 | PubMed
2. **Adler J.** (1966) Chemotaxis in Bacteria. *Science* **153**:708-716 https://doi.org/10.1126/science.153.3737.708 | PubMed
3. **Fu X.,** et al. (2018) Spatial self-organization resolves conflicts between individuality and collective migration. *Nature Communications* **9**:1-12 https://doi.org/10.1038/s41467-018-04539-4 | PubMed
4. **Wolfe A. J.,** Berg H. C. (1989) Migration of Bacteria in Semisolid Agar. *Proc Natl Acad Sci U S A* **86**:6973-6977 https://doi.org/10.1073/pnas.86.18.6973 | PubMed
5. **Zhang Y.,** et al. (2024) Navigated range expansion promotes migratory culling. *Proc Natl Acad Sci U S A* **121**:e2408303121 https://doi.org/10.1073/pnas.2408303121 | PubMed
6. **Cremer J.,** et al. (2019) Chemotaxis as a navigation strategy to boost range expansion. *Nature* **575**:658-663 https://doi.org/10.1038/s41586-019-1733-y | PubMed
7. **Liu W.,** Tokuyasu T. A., Fu X., Liu C. (2021) The spatial organization of microbial communities during range expansion. *Curr Opin Microbiol* **63**:109-116 https://doi.org/10.1016/j.mib.2021.07.005 | PubMed
8. **Bai Y.,** et al. (2021) Spatial modulation of individual behaviors enables an ordered structure of diverse phenotypes during bacterial group migration. *eLife* **10** https://doi.org/10.7554/eLife.67316 | PubMed
9. **Berg H. C.** (2004) *E. coli in motion* Springer-Verlag.
10. **Rosen G.** (1973) Fundamental theoretical aspects of bacterial chemotaxis. *Journal of Theoretical Biology* **41**:201-208 https://doi.org/10.1016/0022-5193(73)90113-6 | PubMed
11. **Sneddon M. W.,** Pontius W., Emonet T. (2012) Stochastic coordination of multiple actuators reduces latency and improves chemotactic response in bacteria. *Proc Natl Acad Sci U S A* **109**:805-810 https://doi.org/10.1073/pnas.1113706109 | PubMed
12. **Wang F. B.,** Yuan J. H., Berg H. C. (2014) Switching dynamics of the bacterial flagellar motor near zero load. *P Natl Acad Sci USA* **111**:15752-15755 https://doi.org/10.1073/pnas.1418548111 | PubMed
13. **Wang F.,** et al. (2017) Non-equilibrium effect in the allosteric regulation of the bacterial flagellar switch. *Nature Physics* **13**:710-714 https://doi.org/10.1038/nphys4081
14. **Waite A. J.,** Frankel N. W., Emonet T. (2018) Behavioral Variability and Phenotypic Diversity in Bacterial Chemotaxis. *Annual Review of Biophysics* **47**:595-616 https://doi.org/10.1146/annurev-biophys-062215-010954 | PubMed
15. **Turner L.,** Berg H. C. (2018) Labeling Bacterial Flagella with Fluorescent Dyes. In: Manson Michael D. (Ed). *Bacterial Chemosensing: Methods and Protocols* Springer New York. pp. 71-76 https://doi.org/10.1007/978-1-4939-7577-8_7 | PubMed
16. **Berg H. C.,** Brown D. A. (1972) Chemotaxis in Escherichia coli analysed by three-dimensional tracking. *Nature* **239**:500-504 https://doi.org/10.1038/239500a0 | PubMed
17. **Frankel N. W.,** et al. (2014) Adaptability of non-genetic diversity in bacterial chemotaxis. *eLife* **3** https://doi.org/10.7554/eLife.03526 | PubMed
18. **Waite A. J.,** et al. (2016) Non - genetic diversity modulates population performance. *Molecular Systems Biology* **12**:895 https://doi.org/10.15252/msb.20167044 | PubMed
19. **Dufour Y. S.,** Gillet S., Frankel N. W., Weibel D. B., Emonet T. (2016) Direct Correlation between Motile Behavior and Protein Abundance in Single Cells. *Plos Computational Biology* **12** https://doi.org/10.1371/journal.pcbi.1005041 | PubMed
20. **Dufour Y.,** Fu X., Hernandez-Nunez L., Emonet T. (2014) Limits of Feedback Control in Bacterial Chemotaxis. *PLoS Computational Biology* **10** https://doi.org/10.1371/journal.pcbi.1003694 | PubMed

21. **Si G.,** Wu T., Qi O., Tu Y. (2012) Pathway-based mean-field model for Escherichia coli chemotaxis. *Physical Review Letters* **109**:0-4 https://doi.org/10.1103/PhysRevLett.109.048101 | PubMed

22. **Vo L.,** et al. (2025) Nongenetic adaptation by collective migration. *Proc Natl Acad Sci U S A* **122**:e2423774122 https://doi.org/10.1073/pnas.2423774122 | PubMed

23. **Mattingly H.,** Emonet T. (2022) Collective behavior and nongenetic inheritance allow bacterial populations to adapt to changing environments. *Proc Natl Acad Sci U S A* **119**:e2117377119 https://doi.org/10.1073/pnas.2117377119 | PubMed

24. **Bhattacharjee T.,** Datta S. (2019) Bacterial hopping and trapping in porous media. *Nat Commun* **10**:2075 https://doi.org/10.1038/s41467-019-10115-1 | PubMed

25. **Bhattacharjee T.,** Datta S. (2019) Confinement and activity regulate bacterial motion in porous media. *Soft Matter* **15**:9920-9930 https://doi.org/10.1039/c9sm01735f | PubMed

26. **Datta A.,** Beier S., Pfeifer V., Grossmann R., Beta C. (2025) Bacterial swimming in porous gels exhibits intermittent run motility with active turns and mechanical trapping. *Sci Rep* **15**:20320 https://doi.org/10.1038/s41598-025-02741-1 | PubMed

27. **Datta A.,** Beta C., Großmann R. (2024) Random walks of intermittently self-propelled particles. *Physical Review Research* **6**:043281 https://doi.org/10.1103/PhysRevResearch.6.043281

28. **Kurzthaler C.,** et al. (2021) A geometric criterion for the optimal spreading of active polymers in porous media. *Nat Commun* **12**:7088 https://doi.org/10.1038/s41467-021-26942-0 | PubMed

29. **Licata N.,** Mohari B., Fuqua C., Setayeshgar S. (2016) Diffusion of Bacterial Cells in Porous Media. *Biophys J* **110**:247-257 https://doi.org/10.1016/j.bpj.2015.09.035 | PubMed

30. **Mattingly H.** (2025) Coarse-graining bacterial diffusion in disordered media to surface states. *Proc Natl Acad Sci U S A* **122**:e2407313122 https://doi.org/10.1073/pnas.2407313122 | PubMed

31. **Wei T.,** et al. (2022) Exploiting spatial dimensions to enable parallelized continuous directed evolution. *Mol Syst Biol* **18**:e10934 https://doi.org/10.15252/msb.202210934 | PubMed

32. **Liu W.,** Cremer J., Li D., Hwa T., Liu C. (2019) An evolutionarily stable strategy to colonize spatially extended habitats. *Nature* **575**:664-668 https://doi.org/10.1038/s41586-019-1734-x | PubMed

33. **Yi X.,** Dean A. (2016) Phenotypic plasticity as an adaptation to a functional trade-off. *eLife* **5**:e19307 https://doi.org/10.7554/eLife.19307 | PubMed

34. **Mohari B.,** et al. (2015) Novel Pseudotaxis Mechanisms Improve Migration of Straight-Swimming Bacterial Mutants Through a Porous Environment. *Mbio* **6**:e00005-15 https://doi.org/10.1128/mBio.00005-15 | PubMed

35. **Jaqaman K.,** et al. (2008) Robust single-particle tracking in live-cell time-lapse sequences. *Nature Methods* **5**:695-702 https://doi.org/10.1038/nmeth.1237 | PubMed

36. **Bertrand T.,** Zhao Y., Benichou O., Tailleur J., Voituriez R. (2018) Optimized Diffusion of Run-and-Tumble Particles in Crowded Environments. *Phys Rev Lett* **120**:198103 https://doi.org/10.1103/PhysRevLett.120.198103 | PubMed

37. **Proverbio D.** (2024) Chemotaxis in heterogeneous environments: A multi-agent model of decentralized gathering past obstacles. *J Theor Biol* **586**:111820 https://doi.org/10.1016/j.jtbi.2024.111820 | PubMed

38. **Rashid S.,** et al. (2019) Adjustment in tumbling rates improves bacterial chemotaxis on obstacle-laden terrains. *P Natl Acad Sci USA* **116**:11770-11775 https://doi.org/10.1073/pnas.1816315116 | PubMed

39. **Pietrangeli T.,** et al. (2025) Universal Law for the Dispersal of Motile Microorganisms in Porous Media. *Phys Rev Lett* **134**:188303 https://doi.org/10.1103/PhysRevLett.134.188303 | PubMed

40. **Keller E.,** Segel L. (1971) Model for chemotaxis. *Journal of Theoretical Biology* **30**:225-234 https://doi.org/10.1016/0022-5193(71)90050-6

41. **Lovely P.,** Dahlquist F. (1975) Statistical measures of bacterial motility and chemotaxis. *J Theor Biol* **50**:477-496 https://doi.org/10.1016/0022-5193(75)90094-6 | PubMed

42. **Tu Y.** (2013) Quantitative modeling of bacterial chemotaxis: signal amplification and accurate adaptation. *Annu Rev Biophys* **42**:337-359 https://doi.org/10.1146/annurev-biophys-083012-130358 | PubMed

43. **Sourjik V.,** Berg H. (2004) Functional interactions between receptors in bacterial chemotaxis. *Nature* **428**:437-441 https://doi.org/10.1038/nature02406 | PubMed

44. **Vladimirov N.,** Lebiedz D., Sourjik V. (2010) Predicted auxiliary navigation mechanism of peritrichously flagellated chemotactic bacteria. *PLoS Comput Biol* **6**:e1000717 https://doi.org/10.1371/journal.pcbi.1000717 | PubMed

45. **Kalinin Y.,** Neumann S., Sourjik V., Wu M. (2010) Responses of Escherichia coli Bacteria to Two Opposing Chemoattractant Gradients Depend on the Chemoreceptor Ratio. *Journal of Bacteriology* **192**:1796-1800 https://doi.org/10.1128/Jb.01507-09 | PubMed

46. **Tu Y.,** Shimizu T., Berg H. (2008) Modeling the chemotactic response of Escherichia coli to time-varying stimuli. *Proc Natl Acad Sci U S A* **105**:14855-14860 https://doi.org/10.1073/pnas.0807569105 | PubMed

47. **Shimizu T. S.,** Tu Y., Berg H. C. (2010) A modular gradient - sensing network for chemotaxis in Escherichia coli revealed by responses to time - varying stimuli. *Molecular systems biology* **6**:382 https://doi.org/10.1038/msb.2010.37 | PubMed

48. **Long J.,** Zucker S., Emonet T. (2017) Feedback between motion and sensation provides nonlinear boost in run-and-tumble navigation. *PLoS Computational Biology* **13**:1-25 https://doi.org/10.1371/journal.pcbi.1005429 | PubMed

49. **Bhattacharjee T.,** Datta S. (2019) Bacterial hopping and trapping in porous media. *Nature Communications* **10**:2075 https://doi.org/10.1038/s41467-019-10115-1 | PubMed

50. **Zhu J.,** Chu P., Fu X. (2025) Understanding the development of bacterial colony: Physiology new technology, and modeling. *Quantitative Biology* **13**:e95 https://doi.org/10.1002/qub2.95 | PubMed

51. **Chu P.,** Zhu J., Ma Z., Fu X. (2025) Colony pattern multistability emerges from a bistable switch. *Proc Natl Acad Sci U S A* **122**:e2424112122 https://doi.org/10.1073/pnas.2424112122 | PubMed

52. **Liu S.,** Fan Y., Belabbas M.-A. (2019) Affine Geometric Heat Flow and Motion Planning for Dynamic Systems. *IFAC-PapersOnLine* **52**:168-173 https://doi.org/10.1016/j.ifacol.2019.11.773

Peer reviews

Reviewer #1 (Public review):

In this manuscript, the authors study optimal chemotactic navigation of bacteria in disordered environments. Most previous work has studied bacterial chemotaxis in free liquid, but navigation in obstructed environments is gaining more attention. Here, the authors first used the classic swim plate assay to select E. coli for chemotaxis in soft agar at two agar concentrations. In the higher concentration, they observed that the population's migration speed increased and the mean run duration decreased over selection cycles. Importantly, the growth rate did not change, so the change in migration speed was due to improved chemotaxis. Then, using a strain in which they could control the mean run duration with an inducible promoter, they measured population migration speed as a function of mean run duration, observing a peak. In liquid, theory predicts a peak when the run duration is comparable to the time scale of rotational diffusion. Here, the peak is at a much shorter run duration, and the optimal run duration decreased with agar concentration. A key feature in previous studies of bacterial motion in obstructed environments has been the dynamics of cell trapping and escape via tumbling. By directly visualizing the flagella in single cells, the authors found that the majority of trap events in semisolid agar did not end with a tumble. This is important because it means that the peak in the migration speed has a different origin from the peak typically seen in the diffusion coefficient, which is due to a balance between longer runs and less time spent trapped. Instead, using a minimal

theoretical model, the authors argue that the peak in the migration speed is due to a balance between longer runs, which improve chemotaxis, and having those runs terminate with a tumble rather than a trap event, because runs that end with trapping do not result in up-gradient bias. Qualitatively similar behavior is seen in simulations of a more complex model of chemotaxis.

Overall, we find the results to be significant and the evidence to be strong. We have some comments, which the authors need to address to improve/clarify their work:

(1) The authors' model predicts that, because cells spontaneously escape traps without tumbling, the diffusion coefficient should depend monotonically on mean run length even though the chemotaxis coefficient is non-monotonic. It would strengthen the paper if the authors could show this to be true in experiments. Part of the reason for this comment is that the flagella labeling experiments were done in agar that was rapidly cooled in a freezer and then thawed, whereas the migration experiments were performed in agar cooled at room temperature. Our (anecdotal) understanding is that the cooling rate dramatically affects the properties of the agar mesh. Verifying that diffusivity is monotonic in mean run length would therefore show that cells' spontaneous escape from traps is not an artifact of the cooling protocol.

(2) Two agar densities were used in their study (0.2%, 0.3%). As shown in Figure 1, while cells in the 0.3% agar showed significant improvements during the directed evolutionary experiments, the cells in 0.2% agar didn't. Correspondingly, the evolved average run time did not show significant changes in the 0.2% agar, but it decreased in the 0.3% agar. What is the reason for this difference? Does it mean the cells are already optimized for the 0.2% agar medium?

(3) Related to the previous comment, the comparison between Figure 1 and Figure 2 should be made clearer. In Figure 2, a peak performance at an intermediate run time is shown, with the optimal run time decreasing with the agar density. Qualitatively, this result, i.e., the existence of the peak performance, gives the evolution experiments shown in Figure 1 a nice explanation. However, quantitatively, the run times shown in Figures 1 and 2 are quite different. For example, for the 0.3% agar case, the change of run time decreases from ~0.6sec. in cycle-1 to ~0.4sec in cycle-40. However, in Figure 2, the optimal run time is ~0.9sec., which means that the migration speed would decrease if the run time is decreased from 0.6sec to 0.4sec. We understand this may only be considered as a qualitative result. However, it does raise the question of what the molecular mechanisms are that drive the directed evolution, which the authors should address.

(4) In Figure 3B, the distributions of speed in different media (liquid versus agar) for cells with bundled and split flagella are shown. While the distribution for the bundled flagella shows nicely the emergence of the trapped state (peak near zero speed), the distribution for the split flagella shows a significant shift of the distribution. Does this mean the agar medium also changes the tumble state significantly? In fact, we are puzzled by the observation that in bulk liquid, the run speed distribution for cells with split flagella seems to be quite similar to that of cells with bundled flagella, which might indicate problems in determining run speed.

(5) Finally, none of the points plotted have error bars. Error bars would allow the readers to evaluate i) whether the changes in mean run speed during selection are significantly resolved and ii) whether the peaks in the migration speeds are significantly resolved.

https://doi.org/10.7554/eLife.110412.1.sa2

Reviewer #2 (Public review):

Summary:

The manuscript by Bai and colleagues investigates how Escherichia coli navigates and explores agar gels through chemotaxis and what parameters of bacterial swimming are tuned under selection pressure for rapid migration (i.e., reaching the edge of the agar plate quickly). Prior studies have examined related questions to a substantial degree. Examples include "Migration of Chemotactic Bacteria in Soft Agar: Role of Gel Concentration" (*https://pmc.ncbi.nlm.nih.gov/articles/PMC3145277*) and numerous other studies in this area (e.g., "Migration of bacteria in semi-solid agar" *https://www.pnas.org/doi/10.1073/pnas.86.18.6973*). From such studies has emerged the paradigm/model that reorientation (i.e., tumbling) is essential when bacteria navigate agar, which is considered a model for "complex" environments, because run-only bacteria become trapped in the agar matrix and are unable to migrate far. This new manuscript provides some evidence that this paradigm may be overly simplified or incomplete. As I understand it, the authors propose that migration is influenced to a greater extent by bias in the chemotactic run, where runs up attractant gradients are longer. The authors incorporate these data into a new model for chemotactic navigation and claim that this work establishes a general principle for how bacteria optimize active transport through complex environments.

I will first note to the editor and authors that I am not qualified to assess the detailed mathematics of the model, and my review therefore focuses on the biology and phenotypes described. Nevertheless, in my view, this manuscript, in its current form, has several important limitations. For each point, I provide suggestions for additional experiments that could strengthen the rigor of the work and clarify the claims.

Strengths:

A strength of this work is the use of microscopy and automated methods to characterize an extremely large number of bacterial cells, which strengthens the authors' claims. However, substantially greater detail on these approaches is needed for the analysis to be reproducible and to allow verification that the analyses were performed correctly.

Weaknesses:

Major concerns

(1) Claims are overly broad, and the experimental system is too artificial to support general conclusions about bacteria, chemotaxis, or evolution.

E. coli MG1655 is a longstanding model organism in the chemotaxis field, and agar chemotaxis assays are also widely used. However, the authors make very broad claims about how phenotypic changes observed during selection in 0.2% or 0.3% agar relate to bacterial chemotaxis and evolution more generally. In essence, the experimental foundation on which the authors build a complex theoretical framework is limited to a domesticated laboratory strain of E. coli and a highly artificial environment consisting of agar in a Petri dish. Although E. coli is well studied, its motility and taxis behaviors are not necessarily representative of bacteria across nature. In addition, natural environments are dynamic, and bacteria rarely experience stable gradients for extended periods, such as the 24-hour time-frame used here. The authors have also only focused on responses to attractant gradients with undefined complex growth media, and not assessed if this is also true for repellent gradients. This is important to consider because E. coli also generates repellent gradients (indole) that are not considered here. E. coli also generates AI-2, sensed as an attractant, that would be an opposing force for migration. For these reasons, it is not clear that the data and theory presented here generalize to diverse bacterial species, to natural environments, or to chemotaxis broadly.

The authors should acknowledge that further work is needed to generalise their findings by testing additional organisms, such as non-laboratory E. coli isolates, other enteric bacteria,

and species with fundamentally different motility systems (e.g., Campylobacter jejuni). Further work could also expand beyond agar by examining chemotaxis in a biological matrix such as mucin, as well as testing responses to defined attractants and repellents.

(2) No genetic component is identified, so claims about evolution are not supported.

Evolution requires heritable genetic changes that produce phenotypes advantageous under a given selection pressure. The authors state that bacteria were selected for rapid migration and that this selection produced progressively more efficient migrators. However, no sequencing analyses of the evolved isolates were performed, no genetic changes were identified, and no mechanism underlying this phenotypic shift was described. Without identifying genetic alterations, they cannot substantiate the claim that evolution occurred. Whole-genome sequencing of the evolved isolates is necessary to determine whether specific mutations underlie the observed phenotypes.

(3) The predictive power of the model is not tested.

The authors develop a model with post-dictive capability, meaning the model reproduces behaviors similar to those observed in the data used to construct it. However, the manuscript does not demonstrate that the model has predictive power. Demonstrating predictive performance would substantially increase the value of the model. For example, the authors could perform an additional round of selection and predict the resulting bacterial behavior under a condition not used during model construction (such as a different agar concentration or predicting the behavior of different bacteria). Otherwise, the authors should tone down the claims.

(4) Limited novelty and impact of the environmental difference studied.

A central point of the manuscript is the difference between evolution in 0.2% versus 0.3% agar and how this difference relates to the proposed model. However, this represents a relatively minor change in the environment experienced by the bacteria. Developing an extensive theoretical framework and proposing that bacterial evolution is highly sensitive to these parameters based on this narrow experimental system may be premature. This would be addressed by the suggested broadening of experiments described above.

(5) The manuscript is too brief, and some data and methods are insufficiently described, particularly related to the machine learning analysis.

The manuscript addresses a complex topic, yet the main text, methods, and figures are very brief, which need not be the case. As a result, it is often difficult to understand exactly what was done and how the data support the authors' claims. More detailed descriptions of the experimental approaches and analyses are necessary.

One example is the machine learning approach used for cell tracking. This method is only briefly described, and no validation data are presented that would allow readers to evaluate whether the approach performs accurately. If the method is robust, it would be a powerful analytical tool, but the current description does not provide sufficient information to evaluate the reliability of the results. This issue is particularly important because the authors conclude that tumbles account for less than 3% of escape events, which contrasts with previous paradigms. Automated tracking methods can be susceptible to artifacts, and therefore, rigorous validation of the tracking pipeline, supported by appropriate figures and benchmark data, is essential.

https://doi.org/10.7554/eLife.110412.1.sa1

Reviewer #3 (Public review):

The manuscript by Bai et al presents a study of the effect of trapping on the efficiency of chemotactic spreading. While the overall impression of the study is positive, there are multiple drawbacks that accumulate and together make the statement of the paper not fully justifiable. Below, I provide some detailed comments in chronological order, and indicate those of particular importance.

(1) On the first page of the Introduction, the authors use the following wording: "...how bacteria optimise their intrinsic motility parameters to maximise navigation efficiency". However, it is not shown or known whether they do. In the experiments, the authors fetch the bacteria at the far front and artificially select the ones with shorter run times. The ones at the front could be the effect of heterogeneity of the population rather than an adaptation. Moreover, the authors claim that the selective pressure is via trapping. But this can be due to a multitude of other factors that change with agar concentration, availability of nutrients, osmotic properties of water, etc.

(2) At the beginning of the results section, the authors claim that for both agar concentrations, they observe a progressive increase in chemotactic navigation. I do not see how the data for 0.2 % agar would correspond to that. Migration speed remains flat.

(3) (Important). The authors claim that the mean run speed remained constant. But this is definitely not true, as seen in the plots. The speed of modernity is increasing for both agar conditions. And here it is important to note that the chemotactic drift velocity is proportional to the square of run speed (which is not the case for the formulas in this paper, see comment below). Thus, even smaller changes in v_0 can result in a significant increase in the drift velocity.

(4) (Important). Tumble bias is also significantly increasing in 0.3 agar concentration. While it is not clear from the paper what exactly the tumble bias is, if it is related to the persistence of the turning angle, this also has a linear effect on the chemotactic drift velocity.

(5) (Important). When performing aTc dependence testing, the authors didn't report how other observables of swimming behaviour are changing.

(6) (Very important). I'm not sure that by interfering with Che-Z expression, one does not affect the whole chemotactic circuit, for example, by changing G (in terms of the model) and thus the optimality occurs not due to the agar concentration/traps but due to the perturbations in the circuit. Also, the effect of different % seems to be much more minor compared to the overall induced changes in spreading speed.

(7) (Very important). I was very confused by the statement of the authors about only 3% of traps being exited due to tumble. I don't think this is possible (in a way consistent with the suggested model). Mean free run times (Figure 1C) go down to 0.4 s. Duration of tumbles is 0.3s (Figure S2c), but the duration of traps is longer than tumbles (and a bit shorter than runs). So how can it be that a running cell gets into a trap and only in 3% cases it experiences a tumble? What would be the distribution of run durations if one combines pre-trap+trap_time+post_trap run time - would they still have a mean below 1s?? It really looks like the authors are not able to detect tumbles when bacteria are trapped. Or is there an active mechanism suppressing tumbles when in the trap?

(8) It is not clear what it means that post-tumble angles were uniformly distributed. Does this refer to only trap-associated tumbles? It is known that in the freely swimming e.coli the tumbling angles are not isotropic but have a preference for the forward direction. Is it different in agar conditions?

(9) (Very important) The authors assume an oversimplified model for the chemotactic drift based on biased random walks. As a result, the answer for chemotactic drift velocity has a wrong scaling with run speed. In the linear theory of chemotaxis by de Gennes, the scaling is v_0^2, while the authors use a linear relationship. Thus, the assumption of the simplified model is incorrect. The exact effect of the traps (where no tumbling is happening, and the directional memory is conserved) needs to be properly calculated, for example, in the same de Gennes framework. And I can't say what the result would be from the top of my head because the calculation is, in fact, not too trivial. Thus, the model used is oversimplified, and thus the fact that it shows a non-monotonous relationship with tau_f is of little predictive power.

Taken together, you see that all the key points that are used in the chain of the argument about the optimality are not rock solid and allow for alternative explanations. I think all those either need to be tested explicitly or at least clearly discussed, and the respective conclusions of the paper need to be rephrased. In my view, this work needs major revision.

https://doi.org/10.7554/eLife.110412.1.sa0